Molecular Therapy
Oncolytics
Original Article

Feasibility study of a novel preparation strategy for anti-CD7 CAR-T cells with a recombinant anti-CD7 blocking antibody

Jing Ye,[1] Yujie Jia,[1] Israth Jahan Tuhin,[2] Jingwen Tan,[1] Masuma Akter Monty,[2] Nan Xu,[1] Liqing Kang,[2] Minghao Li,[1] Xiaoyan Lou,[2] Meixia Zhou,[1] Xiaoyan Fang,[1] Jiaqi Shao,[1] Hongjia Zhu,[1] Zhiqiang Yan,[1] and Lei Yu[1]

[1]Institute of Biomedical Engineering and Technology, Shanghai Engineering Research Center of Molecular Therapeutics and New Drug Development, School of Chemistry and Molecular Engineering, East China Normal University, Shanghai 200062, P.R. China; [2]Shanghai Unicar Therapy Bio Medicine Technology Co. Ltd., Shanghai 201612, P.R. China

Although chimeric antigen receptor (CAR) T cell immunotherapy has shown promising significance in B cell malignancies, success against T cell malignancies remains unsatisfactory because of shared antigenicity between normal and malignant T cells, resulting in fratricide and hindering CAR production for clinical treatment. Here, we report a new strategy of blocking the CD7 antigen on the T cell surface with a recombinant anti-CD7 antibody to obtain a sufficient amount of CD7-targeting CAR-T cells for T cell acute lymphoblastic leukemia (T-ALL) treatment. Feasibility was evaluated systematically, revealing that blocking the CD7 antigen with an antibody effectively blocked CD7-derived fratricide, increased the expansion rate, reduced the proportion of regulatory T (Treg) cells, maintained the stem cell-like characteristics of T cells, and restored the proportion of the $CD8^+$ T cell population. Ultimately, we obtained anti-CD7 CAR-T cells that were specifically and effectively able to kill CD7 antigen-positive target cells, obviating the need for complex T cell modifications. This approach is safer than previous methods and provides a new, simple, and feasible strategy for clinical immunotherapies targeting CD7-positive malignant tumors.

INTRODUCTION

T cell malignancies are a group of heterogeneous diseases that reflect the clonal nature of T cells with impaired functions.[1] In particular, T cell acute lymphoblastic leukemia (T-ALL) is a highly invasive hematological malignancy caused by the abnormal proliferation of hematopoietic stem cells.[2] Despite treatment with multidrug chemotherapy regimens, 30% of patients eventually relapse, and fewer than 15% of relapsed patients have an event-free survival time of 3 years.[3,4] In particular, the malignancy of T cell malignant tumors is greater than that of B cell malignant tumors, which makes T-ALL treatment significantly challenging.[5]

Chimeric antigen receptor (CAR) T cell immunotherapy is promising for the treatment of refractory and relapsed B cell acute lymphoblastic leukemia (r/r B-ALL) and the first commercial T cell therapy approved for cancer.[6,7] This success implies that CAR-T cell therapy is very promising for the treatment of T cell malignancies. At present, CD1a, CD5, and CD7 are the major selective target antigens in T-ALL. However, because CD1a expression is characterized in only some subtypes, such as cortical thymocytes, and CD5 expression is low, targeting CD1a or CD5 is not suitable for long-term treatment.[8–12] CD7 is a 40 kDa single-chain glycoprotein that is expressed by T cells and natural killer (NK) cells.[13] Unlike the CD1a and CD5 antigens, CD7 accounts for more than 95% of the dominant expression in T cell leukemias and lymphomas and stably maintains high expression.[8,14] In addition, clinical data have shown that CD7 is continuously expressed on cancerous T cells at higher levels than that on T cells from normal donors and is therefore considered an attractive target for CAR-T cell therapy.[15]

However, it is almost impossible to produce sufficient anti-CD7 CAR-T cells *in vitro* for clinical therapy because of "fratricide."[16] At present, two strategies have been reported to avoid fratricide. One strategy is to knock out CD7 using CRISPR-Cas9 gene editing technology, and the other is to target the CD7 protein with an anti-CD7 single-chain variable fragment (scFv) coupled with an endoplasmic reticulum (ER)/Golgi-retention domain to retain newly synthesized CD7 in the ER or Golgi apparatus. However, both strategies require additional modifications at the DNA level to inhibit the expression of CD7 on the cell membrane, which may introduce unpredictable risk (such as "off-target" effects); moreover, these

Received 30 May 2021; accepted 17 February 2022;
https://doi.org/10.1016/j.omto.2022.02.013.

Correspondence: Lei Yu, Institute of Biomedical Engineering and Technology, Shanghai Engineering Research Center of Molecular Therapeutics and New Drug Development, School of Chemistry and Molecular Engineering, East China Normal University, Shanghai 200062, P.R. China.
E-mail: yulei@nbic.ecnu.edu.cn
Correspondence: Zhiqiang Yan, Institute of Biomedical Engineering and Technology, Shanghai Engineering Research Center of Molecular Therapeutics and New Drug Development, School of Chemistry and Molecular Engineering, East China Normal University, Shanghai 200062, P.R. China.
E-mail: zqyan@sat.ecnu.edu.cn

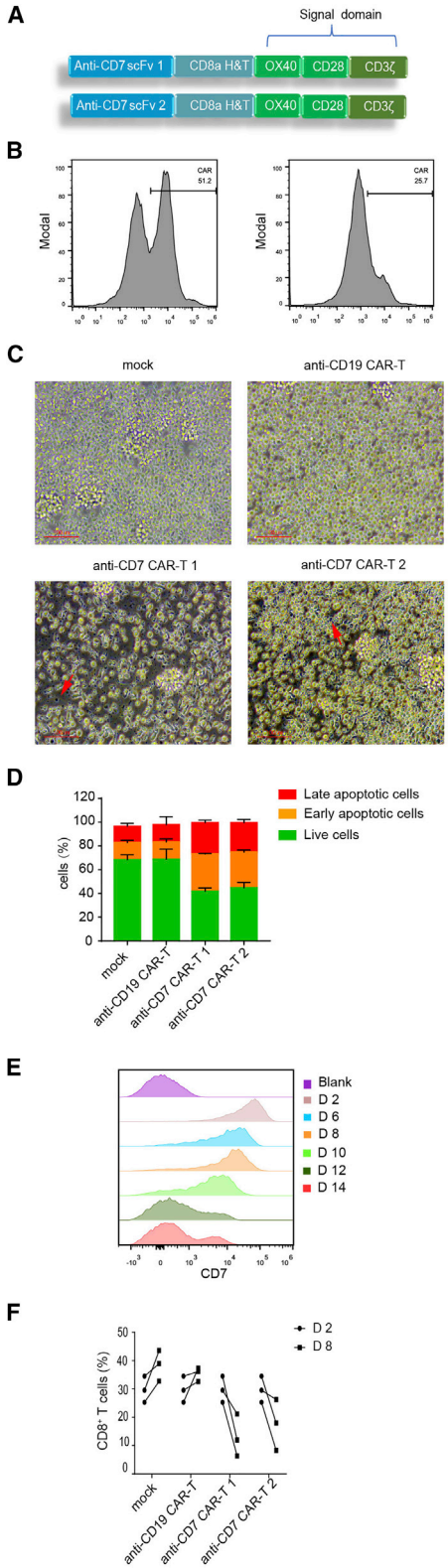

Figure 1. Expression of anti-CD7 CAR on T cells results in fratricide

(A) Schematics of two third-generation anti-CD7 CAR constructs: anti-CD7 CAR-T 1 (top) and anti-CD7 CAR-T 2 (bottom). (B) Representative histograms of anti-CD7 CAR expression in T cells. (C) Cell debris and dead cells in cultures of anti-CD7 CAR-T cells observed under the microscope on day 7. The red arrows represent cell debris or dead cells. Scale bar: 100 μm. (D) Apoptosis in the four cell groups (mock, anti-CD19 CAR-T cells, anti-CD7 CAR-T 1 cells, and anti-CD7 CAR-T 2 cells) on day 8. Data are shown as mean ± SD from triplicate measurements and were visualized using GraphPad Prism. There was no significant difference between the anti-CD7 CAR-T 1 cell and anti-CD7 CAR-T 2 cell, mock, and anti-CD19 CAR-T as well, but the results of the multiple comparison of the late apoptotic cells, early apoptotic cells, and live cells between the anti-CD7 CAR-T 1 cell and mock cells were $p = 0.0044$ (**$p < 0.01$), $p = 0.0002$ (***$p < 0.001$), and $p < 0.0001$ (***$p < 0.001$), respectively. (E) Histograms of CD7 antigen expression on anti-CD7 CAR-T 1 cells from day 2 to day 14. (F) Proportions of $CD8^+$ T cells detected on day 1 and day 8. Data from 3 donors were analyzed and visualized using GraphPad Prism.

strategies may have an unknown impact on the biological function of CAR-T cells because of the lack of CD7 expression on the cell membrane.[10,11,15,17]

Therefore, to overcome the shortcomings of the reported methods for preparing anti-CD7 CAR-T cells, we propose a new strategy in which the CD7 antigen on the T cell surface is blocked with a free anti-CD7 antibody containing the same binding domain as the CAR to avoid fratricide during anti-CD7 CAR-T cell preparation. Our research showed that the anti-CD7 CAR-T cells cultured with the antibody, which was added during the preparation stage, exhibited improved cell viability and proliferation and a relatively ideal subpopulation. Finally, we harvested a sufficient amount of anti-CD7 CAR-T cells with specific and effective cytotoxicity against CD7 antigen-positive target tumor cells for clinical use. This new study provides a simple, safe, and feasible method for preparing anti-CD7 CAR-T cells for the clinical treatment of T-ALL.

RESULTS

The expression of an anti-CD7 CAR on T cells leads to fratricide

To obtain a CAR that can specifically target the CD7 antigen on the surface of tumor cells, we designed two third-generation anti-CD7 CARs (Figure 1A). Anti-CD7 CAR-T 1 and anti-CD7 CAR-T 2 cells were prepared using lentiviral transduction, and the infection efficiencies measured on day 8 were 51.2% and 25.7%, respectively (Figure 1B).

Anti-CD7 CAR-T cells may induce fratricide because of T cell expression of CD7.[15] To explore and confirm this phenomenon, we observed the condition of anti-CD7 CAR-T cells under the microscope and found a large number of dead cells and cell debris in both CAR-T cell groups (Figure 1C). Cell apoptosis results revealed that the proportions of both early and late apoptotic cells in the anti-CD7 CAR-T cell groups were higher than those in the mock group (T cells not transduced with an anti-CD7 CAR) and the anti-CD19 CAR-T cell group, which was used as an irrelevant CAR control (Figure 1D). And the expression of CD25/PD-1 on the anti-CD7 CAR-T cell surface was significantly higher than on the surface of anti-CD19 CAR-T cells, indicating that anti-CD7 CAR-T cells were

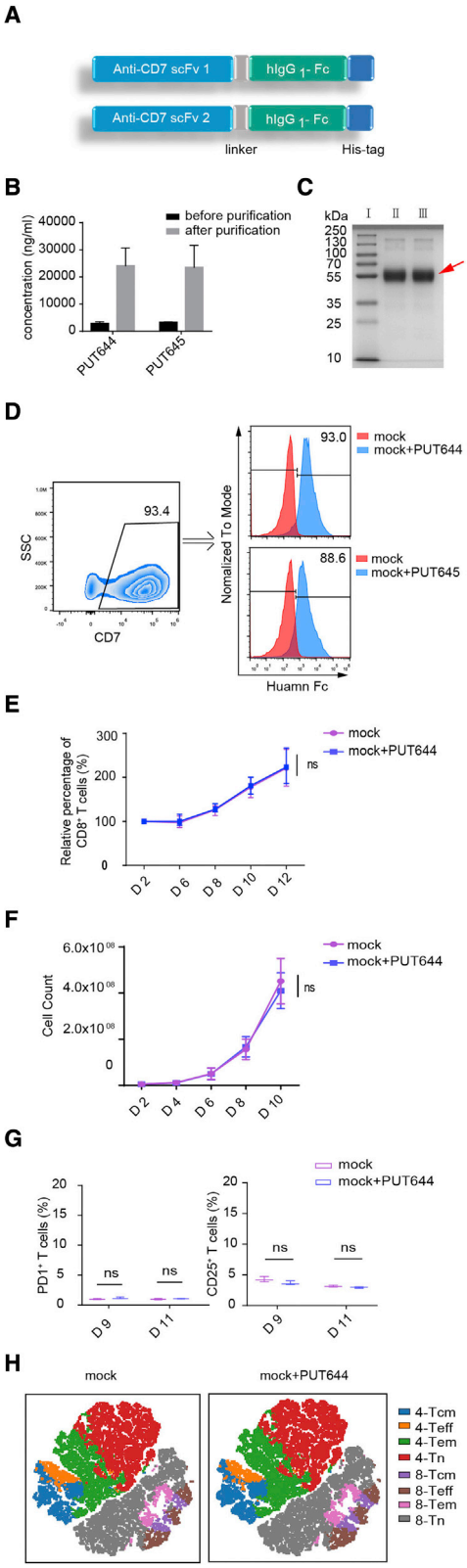

Figure 2. Characterization of anti-CD7 antibodies

(A) Schematic presentation of the PUT644 (top) and PUT645 antibodies (bottom). (B) Before and after purification, the concentrations of the PUT644 and PUT645 antibodies were detected using ELISA. The bar graphs show the mean ± SD from four independent experiments. (C) A protein ladder was used to estimate molecular weight. I, Protein ladder; II, purified PUT644 antibody; III, purified PUT645 antibody. The arrow indicates the corresponding proteins at 55 kDa. (D) The percentage of $CD7^+$ T cells before antibody addition (top) and the percentage of cells combined with the PUT644 antibody (bottom) were determined with an anti-human Fc antibody after incubation for 2 h. (E) The percentage of $CD8^+$ T cells incubated with or without the PUT644 antibody from day 2 to day 12 was detected using fluorescence-activated cell sorting (FACS). The data are shown as mean ± SD from triplicate measurements; $p > 0.05$ (ns). (F) Expansion of T cells with or without an antibody from day 2 to day 10. The bar graphs show the mean ± SD from 3 healthy donors; $p > 0.05$ (ns). (G) CD25 and PD-1 expression on the surface of T cells cultured with or without PUT644 was measured on day 9 and day 11 ($n = 3$ donors; $p > 0.05$; error bars denote the SD). (H) The naive T cell (Tn; $CD45RA^+CCR7^+$), central memory T cell (Tcm; $CD45RA^-CCR7^+$), effector memory T cell (Tem; $CD45RA^-CCR7^-$), and effector T cell (Teff; $CD45RA^+CCR7^-$) subsets of $CD4^+$ and $CD8^+$ T cells as determined using t-distributed stochastic neighbor embedding (tSNE) advanced analysis; the different colors represent individual populations. The data were analyzed at https://premium.cytobank.org/cytobank/login.

highly activated, possibly because of recognition of the target antigen in the culture system (Figure S1A).

For further authentication, CD7 antigen expression was assessed in each group. The corresponding expression in the anti-CD7 CAR-T cell groups was gradually decreased, whereas that in the mock and anti-CD19 CAR-T cell groups remained consistent at day 2 and day 14, respectively (Figures 1E and S1B). Moreover, aberrant phenotypic expression of CD8 was also found in the anti-CD7 CAR-T cell groups compared with both the anti-CD19 CAR-T cell and mock groups (Figure 1F), which was also observed by other researchers.[16]

Therefore, we aimed to improve cell expansion by using antibodies to block the CD7 antigen on the T cell surface and thereby prevent fratricide during the culture process.

Design and characterization of secreted antibodies

Because scFvs are small in size and easily aggregate, they are often fused with an Fc fragment through a hinge region to improve antibody stability.[18,19] Therefore, we ligated the Fc segment sequence of human IgG1 with the scFv 1 sequence (clone m3A1e) or scFv 2 sequence (clone m3A1f) with a structure similar to that of the CAR and added a His-tag sequence to facilitate antibody purification. These constructs were named PUT644 and PUT645, and their theoretical sizes were calculated to be 54.2 and 55.1 kDa, respectively (Figure 2A). The PUT644 and PUT645 antibody concentrations were 24.09 μg/mL and 23.51 μg/mL, respectively (Figure 2B), after purification and concentration. To confirm the identities and purities of the antibodies, we performed SDS-PAGE, and the band estimated at 55 kDa represented the purified antibodies (Figure 2C). To verify whether the prepared antibodies could bind CD7 molecules on the T cell surface, we incubated the antibodies with T cells for 2 h at room temperature. Both soluble antibodies bound to the CD7 antigen; however, the coverage rate of PUT645 on the cell surface was

slightly lower than that of PUT644 (Figure 2D). By comparing the infection efficiency results for CAR-T cells and the antibody characterization results, we chose to use anti-CD7 CAR-T 1 cells and the PUT644 antibody for subsequent experiments.

To verify whether the PUT644 antibody itself could biologically interact with mock T cells, we isolated T cells and cultured them with or without the antibody. Cells were counted and observed for a certain period. Because the $CD8^+$ T cell proportion in the anti-CD7 CAR-T cell group completely differed from that in the anti-CD19 CAR-T cell group, we measured the $CD8^+$ T cell proportion in addition to cell expansion and activation and found no effect of antibody supplementation (Figures 2E and 2G). Then, we stained cells for the markers CD4, CD8, CD45RA, and CCR7 to distinguish naive T lymphocytes (Tn; $CD45RA^+CCR7^+$), central memory T lymphocytes (Tcm; $CD45RA^-CCR7^+$), effector memory T lymphocytes (Tem; $CD45RA^-CCR7^-$), and effector T lymphocytes (Teff; $CD45RA^+CCR7^-$), and none of the cell subgroups was found to be significantly affected (Figure 2H).

Overall, the purified antibody could specifically recognize and block CD7 molecules on the surface of T lymphocytes; did not significantly change the activation, proliferation, or differentiation state of the cells; and had no obvious effect on cell expansion.

Antibodies in the culture medium can slow "fratricide" and promote cell proliferation

Mechanistically, if poor expansion is caused by fratricide, then blocking CD7 antigens on the surface of T cells with a corresponding antibody will improve culture outcomes. We added the PUT644 antibody to the anti-CD7 CAR-T 1 cell culture system at a final concentration of 0.72 μg/mL and named the culture CAR-T 1 + PUT644. At the same time, we prepared a group of anti-CD7 CAR-T 1 cells cultured without the antibody to use as the control. We found that the cell counts between the two groups started to differ on day 6, and anti-CD7 CAR-T cells cultured with the antibody were maximally expanded 83.5-fold (from 2×10^6 to 1.67×10^8) at 10 days post-transduction (Figure 3A). We also calculated the doubling times from cell count data to measure and compare the proliferation rates between the two groups. The doubling time (DT) of the CAR-T 1 + PUT644 group was shortened to at most 56.75% of that of the anti-CD7 CAR-T 1 cell group from day 2 to day 12 ($DT_{[\text{anti-CD7 CAR-T 1}]}$ vs $DT_{[\text{CAR-T 1 + PUT644}]}$ = 123.47 vs 53.41 h) (Figure 3B).

We also verified the cell morphologies and cell apoptosis found that the dead cells and apoptotic cells in the CAR-T 1 + PUT644 group were significantly reduced (Figures 3C and 3D), which was consistent with our cell expansion results. This suggests that the addition of antibodies to the culture medium can alleviate "fratricide" among anti-CD7 CAR-T cells and increase cell expansion.

Antibodies can improve the cell population and reduce exhaustion

Data have shown that cell subsets are related to the clinical response, for example, stem central memory T cells are related to positive cell expansion.[20–23] We found that addition of the antibody increased the Tn cell population but decreased the Treg compared with the non-treated CAR-T cell group, which became more apparent on day 13 (Figure 4A). Considering the differences in cell subpopulations between the two groups, we tested the cytokines in the culture supernatants. We also observed that the IL-10 and IL-6 cytokine levels in the CAR-T 1 + PUT644 group were significantly reduced ($p < 0.0001$ and $p < 0.0001$, respectively), while the IL-4 levels barely differed between the groups (Figure 4B).

After multiple antigen stimulations, T cells can highly express LAG3, TIM3, and other exhaustion markers and gradually lose their effector function.[24] Experimental data showed that the addition of the PUT644 antibody had little effect on the exhaustion marker CTLA4; however, it significantly reduced the expression of TIM3 and LAG3 ($p < 0.0001$ and $p = 0.0107$, respectively) (Figure 4C). This result indicated that the antibody could maintain the cellular effector function to a certain extent and reduce the possibility of exhaustion.

Notably, the addition of the antibody inhibited $CD8^+$ T cell loss (Figure 4D), further indicating that the changed proportion of $CD8^+$ T cells may be unique to anti-CD7 CAR-T cells. Because cell exhaustion can reportedly reduce expansion, we hypothesized that this decline was caused by the impaired expansion capacity of $CD8^+$ T cells because of exhaustion.[25] According to a previous report, after antigen stimulation, T cells enter the pre-exhausted stage and co-express PD-1 and CTLA4, followed by expression of TIM3 and LAG3 in the terminal stage.[24] Therefore, we herein monitored terminal exhausted cell population (i.e., the TIM3 and LAG3 double-positive [$TIM3^+LAG3^+$] cells) and found that the addition of antibodies significantly reduced the proportion of exhausted T cells ($p = 0.0006$). It is worth noting that this reduction was found for both the $CD4^+$ and $CD8^+$ T cell subsets ($p = 0.0142$ and $p < 0.0001$, respectively); however, compared with the $CD4^+$ T cell subset, the $CD8^+$ T cell subset exhibited a larger reduction (Figure 4E).

Therefore, the experimental data suggested that blocking with the antibody yielded cells with more stem cell-like properties, strong cytotoxic capabilities and fewer immunosuppressed and exhaustion features.

Anti-CD7 CAR-T cells cultured with an antibody possess specific and effective cytotoxicity

To measure the killing effect of anti-CD7 CAR-T cells under the new cell culture conditions, we designed *in vitro* cytotoxicity assays. Before all functional assays, cultured CAR-T cells were washed several times to eliminate the influence of any residual antibodies during the experiments.

Cytotoxicity was measured through an enzyme-based LDH assay. CD7-positive Jurkat cell lines were used as target cells, and the expression of the CD7 antigen on the surface of target cells was confirmed using flow cytometry (Figures 5A and S2A). Cells from

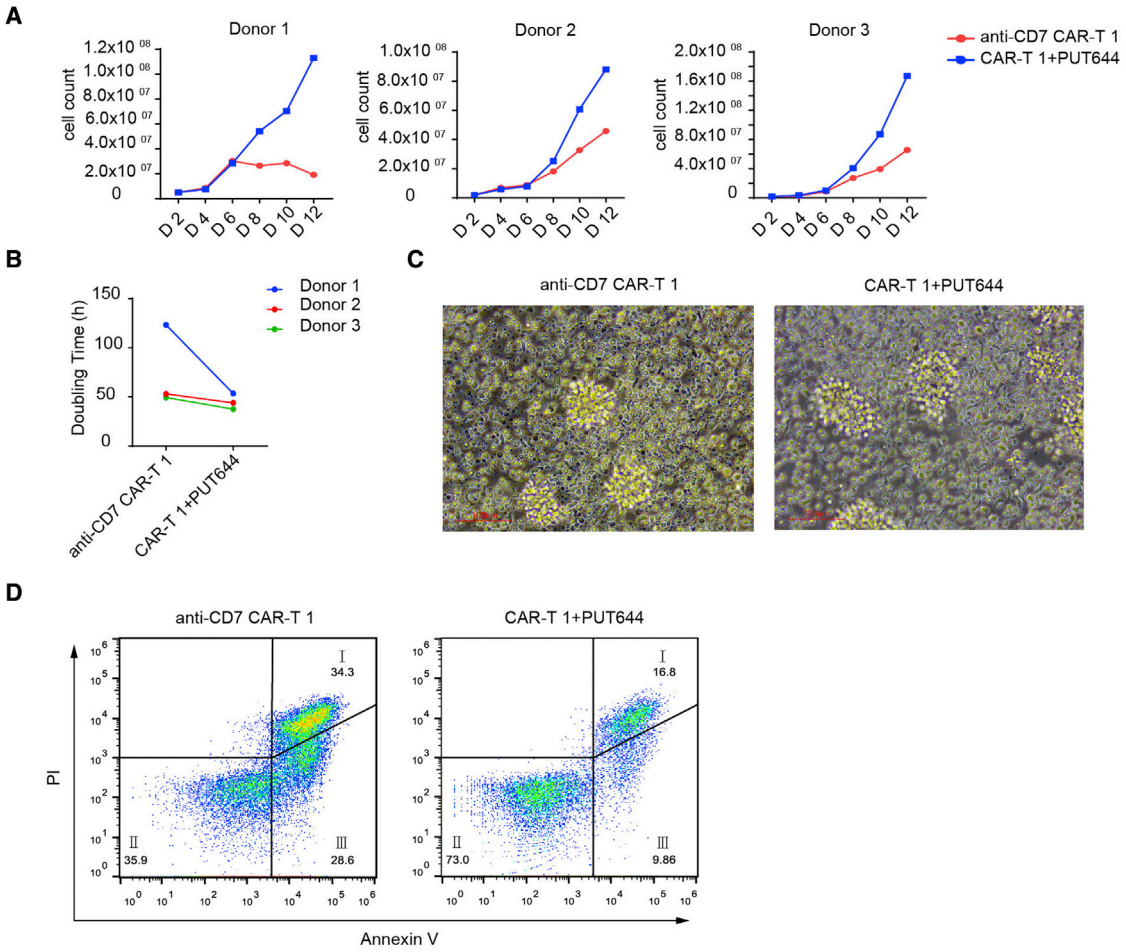

Figure 3. Anti-CD7 CAR-T cells induce fratricide, which is prevented by antibody addition

(A and B) Cell counts plotted from day 2 to day 12 and the doubling time (DT) of cell expansion were analyzed for cells from three donors. DT = 240 × [lg_2/(lgN_{D12} − lgN_{D2})]. (C) Cell debris and dead cells in anti-CD7 CAR-T 1 cultures were observed under a microscope on day 10. Cells were cultured in complete medium in the presence or absence of the PUT644 antibody. Scale bar: 100 μm. (D) Anti-CD7 CAR-T 1 cells cultured with or without the PUT644 antibody were sorted on day 8 for evaluation with Annexin V and PI. Representative cell apoptosis results are shown in plots generated with FlowJo. I, late apoptotic cells; II, live cells; III, early apoptotic cells.

the CAR-T 1 + PUT644 and nontransduced T cell (mock) groups were used as effector cells, and the mock group served as the control. Cytotoxicity assessment revealed that cells from the CAR-T 1 + PUT644 group effectively killed the target cells, while the mock control cells had no cytotoxic effect (Figure 5B).

As the LDH assay measures the cytotoxicity of effector cells at the enzyme level, we further validated the cytotoxic effects at the cellular level. To do this, we measured the percentage of GFP^+ Jurkat cells using flow cytometry (Figures 5C and S2B). The cells were incubated at an effector (E)/target (T) ratio of 1:1 for 18 h, and the percentage of live target cells ($7AAD^-GFP^+$) in the CAR-T 1 + PUT644 group decreased from 51.7% to 16.1% (Figure 5D). Furthermore, the cytotoxic cytokines IFN-γ and TNF produced by CAR-T cells were measured using a corresponding method at E/T ratios of 10:1, 5:1, and 2.5:1, confirming that cells from the CAR-T 1 + PUT644 group released more cytokines than those in the mock group, as anticipated (Figure 5E).

The results demonstrated that anti-CD7 CAR-T cells have the ability to kill CD7-positive tumor cells in an antigen-specific manner.

DISCUSSION

The successful clinical effect of CAR-T cell immunotherapy on B cell malignant tumors is unprecedented, prompting the desire to expand the research progress related to engineered T cells to T cell malignant tumors.[26–28] Concomitantly, CAR-T cells fail to expand because of fratricide, which can lead to restrictions regarding large-scale production and insufficient efficacy.

In addition, two concurrent strategies, CRISPR-Cas9 gene editing technology and ER retention of CD7 molecules, have been used to avoid

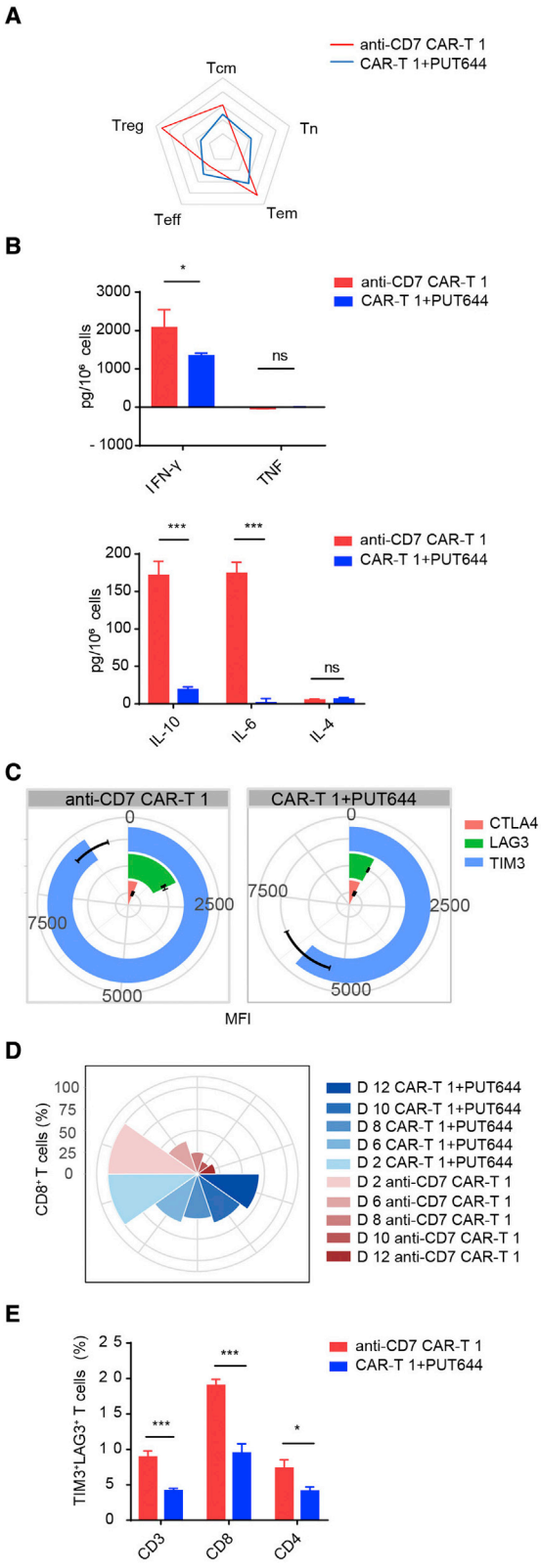

Figure 4. Antibodies can change cell subpopulations and degree of exhaustion

(A) Representative phenotypes of activated CAR-T cells cultured with or without the antibody on day 13. (B) Culture medium supernatants were collected on day 8 and day 10, and the cytokines IFN-γ, TNF, IL-10, IL-6, and IL-4 were detected. C pg/10^6 cells = $10^6 \times (C_{D10} \times VD_{10} - C_{D8} \times V_{D8})/N_{D10}$ (C, concentration of the cytokine; V, cell culture volume; N, cell count). The data are shown as mean ± SD from triplicate measurements (***$p < 0.001$, *$p < 0.05$, and $p > 0.05$ [ns]). (C) The mean fluorescence intensities of the exhaustion markers CTLA4, LAG3, and TIM3 were detected using FACS on day 13; the data shown as mean ± SD from triplicate measurements and were analyzed using Python. The multiple comparison of TIM3, LAG3, and CTLA4 between the anti-CD7 CAR-T cell and CAR-T 1 + PUT644 groups was performed using GraphPad Prism, and the results were $p < 0.0001$ (***$p < 0.001$), $p = 0.0107$ (*$p < 0.05$), and $p = 0.9826$ ($p > 0.05$, ns), respectively. (D) The percentages of $CD8^+$ T cells measured from day 6 to day 12 were normalized to the result detected on day 2. The data are shown using a Nightingale rose chart. (E) Cells were collected on day 11, and the percentage of $LAG3^+TIM3^+$ T cells was detected using FACS. The data are shown as mean ± SD from triplicate measurements (***$p < 0.001$ and *$p < 0.05$).

fratricide, but both methods required additional genetic engineering, which has long-term safety risks.[15,16] Notably, these approaches also increase the difficulty, complexity, and unpredicted toxicity of CAR-T cell therapy.[29] In addition, these strategies cannot yield 100% CD7-negative T cells, and residual CD7-positive T cells still induce fratricide.[16]

In this study, we proposed a simple and effective production strategy in which a recombinant anti-CD7 antibody was constructed and used to block CD7 antigen-derived fratricide. After verification, the expansion of anti-CD7 CAR-T cells cultured with the recombinant antibody may be clinically appropriate for treating B-ALL according to the infusion scale established by Kymriah.[30–32] Following this strategy, the generation of CAR-T cells with robust and specific cytotoxicity against T cell malignancies is more feasible without requiring the extra step of genetic T cell modification.

By using the recombinant anti-CD7 blocking strategy, we obtained not only a sufficient number of anti-CD7 CAR-T cells but also an improved phenotype to enhance the anticancer profile of CAR-T cells. The first is the increased ratio of $CD8^+$ T cells. Activated $CD8^+$ T cells are the main source of CTLs, which have important anti-tumor effects.[33] So the increased proportion of the $CD8^+$ T cell population can improve the cytotoxicity. The second is decreased exhaustion. A clinical study indicated that a constrained CAR-T cell capacity was associated with the continuous expression of exhaustion markers in patients with poor responses to anti-leukemic therapy.[34] Our data showed that addition antibody can decrease the expression of the exhaustion markers to improve the expansion capacity. Further analysis revealed that the percentage of the $TIM3^+$ $LAG3^+$ population of $CD8^+$ T cells was reduced to a significantly greater extent than the $CD4^+$ T cells. Thus, we anticipated that the increased proportion of $CD8^+$ T cells was potentially due to the antibody preferentially inhibiting $CD8^+$ T cell exhaustion.

The third is the improved cell subpopulation. Teff cells are reported to have the greatest cytotoxic effect; however, Tn cells are more

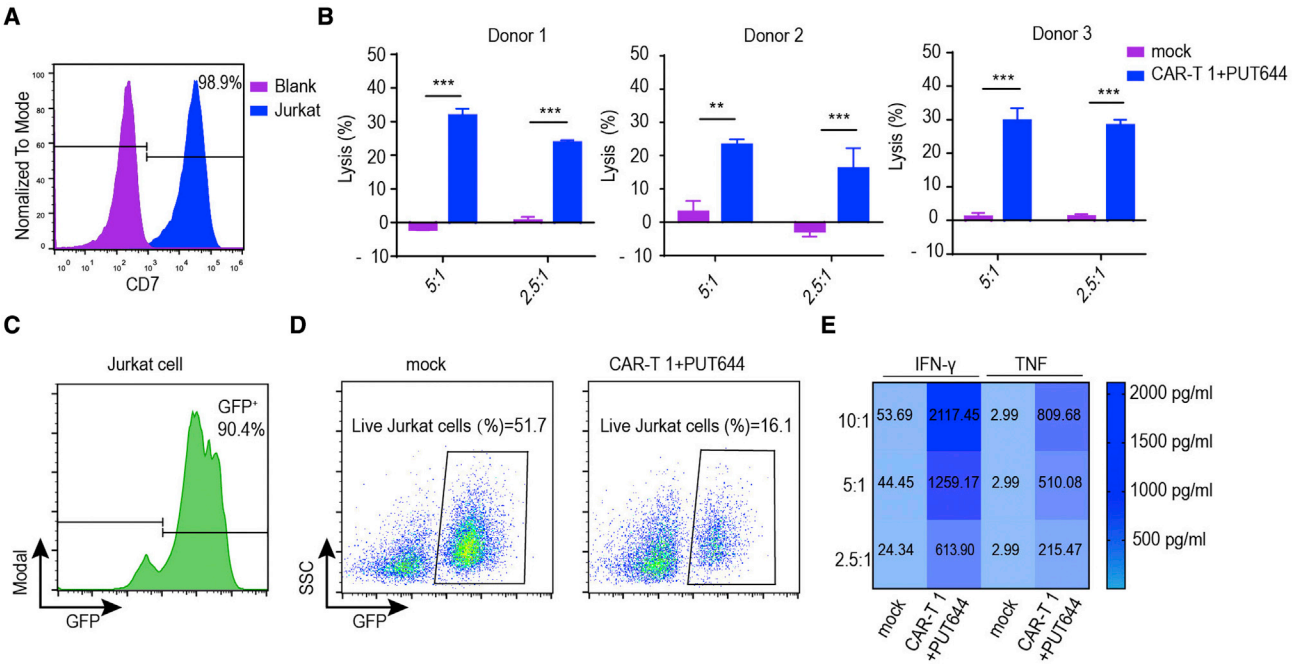

Figure 5. Anti-CD7 CAR-T cells cultured with an antibody possess strong cytotoxicity against CD7-positive tumor cells

(A) Normalized flow cytometric histograms for CD7 expression on Jurkat (positive control) cells. (B) The cytotoxicity of nontransduced T cells (mock) and anti-CD7 CAR-T cells cultured with the PUT644 antibody against target Jurkat cells was evaluated by measuring the amount of LDH released into the culture supernatants using an LDH kit at a wavelength of 490 nm. The bars show the mean ± SD of 24 h cytotoxicity at E/T ratios of 5:1 and 2.5:1. $^{**}p < 0.01$ and $^{***}p < 0.001$. (C) GFP protein expression as detected using flow cytometry. (D) GFP^+ Jurkat cells were coincubated at a 1:1 E/T ratio with mock (nontransduced T cells) or anti-CD7 CAR-T cells (cultured with the PUT644 antibody) for 18 h prior to FACS analysis. The frequency of residual live GFP^+ ($7\text{-}AAD^-GFP^+$) target cells was analyzed using FlowJo. (E) Mock and anti-CD7 CAR-T cells were incubated with Jurkat cells at E/T ratios of 10:1, 5:1, and 2.5:1 for 24 h, and the supernatants were then collected to detect IFN-γ and TNF. The data are shown as a heatmap.

efficacious, as they can self-renew and promote immune reconstitution.[20,21] Moreover, clinical data have shown that the proportion of $CD45RA^+CCR7^+$ T cells in infusions is closely related to the bodily expansion of cells and that the level of Treg cells negatively affects the clinical response to adoptive cancer immunotherapy.[22,35–38] We analyzed the anti-CD7 CAR-T cell subtypes and found that the antibody increased the prevalence of stem cell characteristics and, in addition, decreased the number of Treg cells in the antibody-treated group compared with the nontreated group. Therefore, the addition of the anti-CD7 blocking antibody during the generation of anti-CD7 CAR-T cells might improve persistence and reduce immunosuppression *in vivo*.

In summary, this study is the first to propose an innovative strategy for culturing anti-CD7 CAR-T cells together with an anti-CD7 antibody and included a systematic analysis and evaluation of treatment efficacy in T-ALL. In brief, the findings herein demonstrate that the addition of a blocking antibody to anti-CD7 CAR-T cell therapy can increase cell viability and expansion and, more important, improve cell subsets and decrease cell exhaustion. Therefore, this is a feasible strategy to provide a simple, safe, and cost-effective production method for making a sufficient amount of long-lasting and effective clinical-grade anti-CD7 CAR-T cells for treating T cell malignancies.

MATERIALS AND METHODS

Cell lines and culture conditions

The CD7-positive leukemia cell line Jurkat and the CD7-negative cell line Raji were purchased from the American Type Culture Collection (ATCC; Manassas, VA), and Raji-GFP^+ cells were purchased from Biocytogen (Wakefield, MA). All target cells were cultured with RPMI 1640 medium (Gibco, Grand Island, NY) supplemented with 10% fetal bovine serum (FBS; Biological Industries, Kibbutz Beit-Hashita, Israel) and 1% penicillin streptomycin (Gibco).

For Jurkat-GFP stable cell line preparation, cells were transfected with a plasmid containing a GFP reporter gene using the electroporation method. After electroporation, cells were selected with medium containing an appropriate concentration of puromycin (Yisheng Biotechnology, Shanghai, China) to generate a specific cell line. The HEK293T cell line (ATCC) was cultured with DMEM (Gibco) supplemented with 10% FBS. Cells were maintained at 37°C and 5% CO_2 under fully humidified conditions throughout the experimental period.

CAR plasmid construction

We designed and constructed a third-generation anti-CD7 CAR plasmid containing the following gene sequences (5′ to 3′): an anti-CD7 scFv (clones m3A1e and m3A1f), the transmembrane and hinge

regions of the CD8α molecule, the costimulatory molecules human CD134 (OX40) and human CD28, and the CD3ζ signaling domain.[39] All DNA sequences of gene elements were obtained from the National Center for Biotechnology Information database. Sequences were synthesized by Tsingke Biological Technology (Shanghai, China) and cloned using the PUT plasmid backbone (Unicar-Therapy Biomedicine Technology, Shanghai, China). All plasmids were packaged with a 4-plasmid packaging system, lentiviruses were packaged by transient transfection into HEK293T cells, and the harvested supernatant was stored at −80°C until use.

Antibody production

The anti-CD7 scFv (clones m3A1e and m3A1f) was fused with the constant fragment (Fc) domain of human IgG1, and then the scFv coding sequence was cloned into the expression plasmid by seamless cloning. The plasmid was introduced into HEK293T cells by lentiviral transfection, and the antibody supernatant was collected and purified by affinity chromatography (AFC) on the basis of the combination of the His tag and nickel. Then, the purified solution was concentrated by tangential flow filtration (TFF). To characterize the antibody, 10% SDS-polyacrylamide gel electrophoresis (PAGE) (10% SDS-PAGE Gel ultra-fast preparation kit; Beyotime, Shanghai, China) followed by Coomassie brilliant blue staining was used to analyze antibody purity, and a His tag ELISA Detection kit (GenScript, Piscataway, NJ) was used to detect the antibody concentration.

CAR-T cell construction and preparation

Peripheral blood was collected from donors, and mononuclear cells were isolated with gradient centrifugation using human mononuclear cell separation medium (Oriental Hua Hui, Beijing, China). Further $CD4^+$ and $CD8^+$ T cell subtypes were isolated using the positive selection magnetic microbead cell separation method (Miltenyi Biotec, Bergisch Gladbach, Germany). At 24 h prior to transduction, which was considered day 1, isolated T cells were stimulated with anti-CD3/CD28 monoclonal antibodies (Miltenyi Biotec). Then the cells were transduced with a lentivirus for anti-CD7 CAR transduction for 48 h. The cells were cultured and maintained in AIM-V medium (Gibco) supplemented with 1000 IU/mL recombinant human IL-2 (PeproTech, Rocky Hill, NJ) and 5% FBS (Gibco). Additionally, an anti-CD7 antibody (PUT644 or PUT645) was added to prevent autolysis after CAR transduction via the recognition of transduced CD7 CAR and intrinsic CD7 and was maintained until further analysis. Fresh complete medium and the anti-CD7 antibody were added every 1–2 days, and the cells were maintained at a density of 5×10^5/mL at 37°C and 5% CO_2. Before all coculture or functional studies, the cells were washed thoroughly with PBS to remove any residual antibody.[40]

Flow cytometry

All cells harvested for flow cytometric analysis were washed two times with PBS supplemented with 1% FBS (Biological Industries). The anti-CD7 CAR-T cell infection efficiency was detected using FITC-labeled recombinant protein L (ACRO, Newark, DE). The added antibodies PUT644 and PUT645 were detected by staining with a PE-conjugated anti-human IgG Fc antibody (BioLegend, San Diego, CA). To detect the degree of cell activation, we used FITC-conjugated anti-human CD25 (BioLegend), APC-conjugated anti-human CD25 (BD Pharmingen, San Diego, CA), and PerCP/Cyanine5.5-conjugated anti-human CD279 (PD-1) (BioLegend) antibodies. The $CD4^+/CD8^+$ T cell ratio was measured using a PerCP/Cyanine5.5-conjugated anti-human CD4 antibody (BioLegend) or PE/Cyanine7-conjugated anti-human CD4 antibody (BioLegend) and an APC/Cyanine7-conjugated anti-human CD8 antibody (BioLegend) or anti-CD8a monoclonal antibody (SK1) conjugated to PE (eBioscience, San Diego, CA). The T cell subpopulation was stained with an Alexa Fluor 700-conjugated anti-CD4 monoclonal antibody (eBioscience) and APC/Cyanine7-conjugated anti-human CD8 antibody (BioLegend). A PE-conjugated anti-human CD197 (CCR7) antibody (BioLegend), PerCP/Cyanine5.5-conjugated anti-human CD45RA antibody (BioLegend), PE-Cyanine7-conjugated CD127 monoclonal antibody (eBioscience), and FITC-conjugated anti-human CD25 antibody (BioLegend) were also used. The detection antibodies used to characterize T lymphocyte exhaustion were as follows: an Alexa Fluor 700-conjugated anti-CD4 monoclonal antibody (eBioscience), an APC/Cyanine7-conjugated anti-human CD8 antibody (BioLegend), a FITC-conjugated anti-CD223 (LAG-3) monoclonal antibody (eBioscience), a PE-conjugated mouse anti-human TIM-3 (CD366) antibody (BD Pharmingen), and a PE-Cyanine7-conjugated anti-CD152 (CTLA-4) monoclonal antibody (eBioscience). To detect the degree of cell apoptosis, we stained cells according to the instructions for the Annexin V-FITC Apoptosis Detection Kit (Beyotime). All samples were run on an Attune NxT flow cytometer (Thermo Fisher Scientific, Waltham, MA), and data were analyzed using FlowJo version 10 software (TreeStar, San Carlos, CA).

Lactate dehydrogenase cytotoxicity assay

To measure the cytotoxicity of anti-CD7 CAR-T cells, a lactate dehydrogenase (LDH) cytotoxicity assay was used. Effector cells were harvested and washed with PBS several times to remove any residual anti-CD7 antibody. Afterward, effector cells (anti-CD7 CAR-T cells) and target cells (Jurkat or Raji cells) were cocultured, and the supernatant was collected to measure the amount of LDH released. During the experiment, effector and target cells were plated at E/T ratios of 5:1 and 2.5:1, respectively. The cells were assayed in triplicate wells of a 96-well plate in AIM-V medium supplemented with 4% FBS (Gibco) for 24 h. Cytotoxicity was measured using the Cytotoxicity Detection Kit (Promega, Madison, WI) according to the manufacturer's protocol. Released LDH was detected at 490 nm using a Multiskan GO (Thermo Fisher Scientific) spectrophotometer, and cytotoxicity was calculated using the following formula: % lysis = (experimental LDH release − spontaneous LDH release)/(maximum LDH release − spontaneous LDH release) × 100.

FL-cytotoxicity assay

On day 14, we co-cultured anti-CD7 CAR-T cells with Jurkat-GFP or Raji-GFP target cells at an E/T ratio of 1:1 in triplicate. Cells were incubated for 18 h in a total volume of 100 μL AIM-V medium (Gibco) supplemented with 4% FBS (Gibco). Raji-GFP cells were

used as a negative control. Samples were stained with 7-AAD according to the manufacturer's instructions and run on an Attune NxT flow cytometer. Data were analyzed with FlowJo version 10 software.

Cytokine release assay

Effector cells and target cells were plated at E/T ratios of 10:1, 5:1, and 2.5:1 for 18 h, and then the supernatants were collected in separate wells of a plate for detection. Cytokines (IL-2, IL-4, IL-6, IL-10, IFN-γ, TNF, and IL-17A) were measured using the Human Th1/Th2/Th17 Cytometric Bead Array (CBA) Kit (BD Bioscience) following the manufacturer's instructions. Data were analyzed using LEGENDplex version 8.0.

Statistical analysis

Data from *in vitro* experiments were statistically analyzed and plotted using GraphPad Prism 8.0 (GraphPad Software, San Diego, CA). Data acquired from *in vitro* assays performed in replicates (n = 3 or 4) are presented as mean ± SD unless indicated otherwise. The activation, cytokine secretion, and exhaustion detection assay results were analyzed using two-way ANOVA. The findings were defined as either not significant (ns; $p > 0.05$) or significant at $^{*}p < 0.05$, $^{**}p < 0.01$, or $^{***}p < 0.001$, and significance is indicated above the figure panels or in the figure legends.

SUPPLEMENTAL INFORMATION

Supplemental information can be found online at https://doi.org/10.1016/j.omto.2022.02.013.

ACKNOWLEDGMENTS

We are particularly grateful to Jing Wang, and we thank to Zhou Yu, Linjie Xu, Kuan Li, Yi Xia, Guilin Nie, and others for their support. This work was supported by The National Natural Science Foundation of China (No.81872812 and No.82073800).

AUTHOR CONTRIBUTIONS

L.Y., Z.Y., and J.Y. designed the research and controlled the project schedule. Y.J., I.J.T., and J.Y. conducted experiments and obtained data. J.Y. analyzed the data, drew pictures, and wrote article. Y.J., I.J.T., M.Z., M.A.M., and others were responsible for revision of the manuscript. X.F., J.T., and others collected relevant materials. All authors read and approved the final manuscript.

DECLARATION OF INTERESTS

The authors declare no competing interests.

REFERENCES

1. Scherer, L.D., Brenner, M.K., and Mamonkin, M. (2019). Chimeric antigen receptors for T-cell malignancies. Front. Oncol. *9*, 126.
2. Belver, L., and Ferrando, A. (2016). The genetics and mechanisms of T cell acute lymphoblastic leukaemia. Nat. Rev. Cancer *16*, 494–507.
3. Rodriguez, S., Abundis, C., Boccalatte, F., Mehrotra, P., Chiang, M.Y., Yui, M.A., Wang, L., Zhang, H., Zollman, A., Bonfim-Silva, R., et al. (2020). Therapeutic targeting of the E3 ubiquitin ligase SKP2 in T-ALL. Leukemia *34*, 1241–1252.
4. Vadillo, E., Dorantes-Acosta, E., Pelayo, R., and Schnoor, M. (2018). T cell acute lymphoblastic leukemia (T-ALL): new insights into the cellular origins and infiltration mechanisms common and unique among hematologic malignancies. Blood Rev. *32*, 36–51.
5. Fleischer, L.C., Spencer, H.T., and Raikar, S.S. (2019). Targeting T cell malignancies using CAR-based immunotherapy: challenges and potential solutions. J. Hematol. Oncol. *12*, 141.
6. Schuster, S.J., Bishop, M.R., Tam, C.S., Waller, E.K., Borchmann, P., McGuirk, J.P., Jäger, U., Jaglowski, S., Andreadis, C., Westin, J.R., et al. (2019). Tisagenlecleucel in adult relapsed or refractory diffuse large B-cell lymphoma. New Engl. J. Med. *380*, 45–56.
7. Neelapu, S.S., Locke, F.L., Bartlett, N.L., Lekakis, L.J., Miklos, D.B., Jacobson, C.A., Braunschweig, I., Oluwole, O.O., Siddiqi, T., Lin, Y., et al. (2017). Axicabtagene ciloleucel CAR T-cell therapy in refractory large B-cell lymphoma. New Engl. J. Med. *377*, 2531–2544.
8. Sanchez-Martinez, D., Baroni, M.L., Gutierrez-Aguera, F., Roca-Ho, H., Blanch-Lombarte, O., Gonzalez-Garcia, S., Torrebadell, M., Junca, J., Ramirez-Orellana, M., Velasco-Hernandez, T., et al. (2019). Fratricide-resistant CD1a-specific CAR T cells for the treatment of cortical T-cell acute lymphoblastic leukemia. Blood *133*, 2291–2304.
9. Mamonkin, M., Rouce, R.H., Tashiro, H., and Brenner, M.K. (2015). A T-cell-directed chimeric antigen receptor for the selective treatment of T-cell malignancies. Blood *126*, 983–992.
10. Gomes-Silva, D., Atilla, E., Atilla, P.A., Mo, F., Tashiro, H., Srinivasan, M., Lulla, P., Rouce, R.H., Cabral, J.M.S., Ramos, C.A., et al. (2019). CD7 CAR T cells for the therapy of acute myeloid leukemia. Mol. Ther. *27*, 272–280.
11. Gomes-Silva, D., Srinivasan, M., Sharma, S., Lee, C.M., Wagner, D.L., Davis, T.H., Rouce, R.H., Bao, G., Brenner, M.K., and Mamonkin, M. (2017). CD7-edited T cells expressing a CD7-specific CAR for the therapy of T-cell malignancies. Blood *130*, 285–296.
12. Cooper, M.L., and DiPersio, J.F. (2019). Chimeric antigen receptor T cells (CAR-T) for the treatment of T-cell malignancies. Best Pract. Res. Clin. Haematol. *32*, 101097.
13. Stillwell, R., and Bierer, B.E. (2001). T cell signal transduction and the role of CD7 in costimulation. Immunologic Res. *24*, 31–52.
14. Campana, D., van Dongen, J.J., Mehta, A., Coustan-Smith, E., Wolvers-Tettero, I.L., Ganeshaguru, K., and Janossy, G. (1991). Stages of T-cell receptor protein expression in T-cell acute lymphoblastic leukemia. Blood *77*, 1546–1554.
15. Png, Y.T., Vinanica, N., Kamiya, T., Shimasaki, N., Coustan-Smith, E., and Campana, D. (2017). Blockade of CD7 expression in T cells for effective chimeric antigen receptor targeting of T-cell malignancies. Blood Adv. *1*, 2348–2360.
16. Cooper, M.L., Choi, J., Staser, K., Ritchey, J.K., Devenport, J.M., Eckardt, K., Rettig, M.P., Wang, B., Eissenberg, L.G., Ghobadi, A., et al. (2018). An "off-the-shelf" fratricide-resistant CAR-T for the treatment of T cell hematologic malignancies. Leukemia *32*, 1970–1983.
17. Tsai, S.Q., and Joung, J.K. (2016). Defining and improving the genome-wide specificities of CRISPR-Cas9 nucleases. Nat. Rev. Genet. *17*, 300–312.
18. Moutel, S., El Marjou, A., Vielemeyer, O., Nizak, C., Benaroch, P., Dübel, S., and Perez, F. (2009). A multi-Fc-species system for recombinant antibody production. BMC Biotechnol. *9*, 14.
19. Zou, H., Tuhin, I.J., Monty, M.A., Luo, S., Shao, J., Yan, Z., and Yu, L. (2020). Gene therapy for hepatocellular carcinoma using adenoviral vectors delivering a gene encoding IL-17a-neutralizing antibody fragments. Hum. Gene Ther. *31*, 1074–1085.
20. Klebanoff, C.A., Gattinoni, L., and Restifo, N.P. (2012). Sorting through subsets: which T-cell populations mediate highly effective adoptive immunotherapy? J. Immunother. *35*, 651–660.
21. Stock, S., Schmitt, M., and Sellner, L. (2019). Optimizing manufacturing protocols of chimeric antigen receptor T cells for improved anticancer immunotherapy. Int. J. Mol. Sci. *20*, 6223.
22. Xu, Y., Zhang, M., Ramos, C.A., Durett, A., Liu, E., Dakhova, O., Liu, H., Creighton, C.J., Gee, A.P., Heslop, H.E., et al. (2014). Closely related T-memory stem cells correlate with in vivo expansion of CAR.CD19-T cells and are preserved by IL-7 and IL-15. Blood *123*, 3750–3759.
23. Yao, X., Ahmadzadeh, M., Lu, Y.C., Liewehr, D.J., Dudley, M.E., Liu, F., Schrump, D.S., Steinberg, S.M., Rosenberg, S.A., and Robbins, P.F. (2012). Levels of peripheral

CD4(+)FoxP3(+) regulatory T cells are negatively associated with clinical response to adoptive immunotherapy of human cancer. Blood *119*, 5688–5696.

24. Ando, M., Ito, M., Srirat, T., Kondo, T., and Yoshimura, A. (2020). Memory T cell, exhaustion, and tumor immunity. Immunological Med. *43*, 1–9.
25. Kasakovski, D., Xu, L., and Li, Y. (2018). T cell senescence and CAR-T cell exhaustion in hematological malignancies. J. Hematol. Oncol. *11*, 91.
26. Brentjens, R.J., Davila, M.L., Riviere, I., Park, J., Wang, X., Cowell, L.G., Bartido, S., Stefanski, J., Taylor, C., Olszewska, M., et al. (2013). CD19-targeted T cells rapidly induce molecular remissions in adults with chemotherapy-refractory acute lymphoblastic leukemia. Sci. translational Med. *5*, 177ra38.
27. Maude, S.L., Frey, N., Shaw, P.A., Aplenc, R., Barrett, D.M., Bunin, N.J., Chew, A., Gonzalez, V.E., Zheng, Z., Lacey, S.F., et al. (2014). Chimeric antigen receptor T cells for sustained remissions in leukemia. New Engl. J. Med. *371*, 1507–1517.
28. Turtle, C.J., Hanafi, L.-A., Berger, C., Gooley, T.A., Cherian, S., Hudecek, M., Sommermeyer, D., Melville, K., Pender, B., Budiarto, T.M., et al. (2016). CD19 CAR-T cells of defined CD4+:CD8+ composition in adult B cell ALL patients. J. Clin. Invest. *126*, 2123–2138.
29. Kimberland, M.L., Hou, W., Alfonso-Pecchio, A., Wilson, S., Rao, Y., Zhang, S., and Lu, Q. (2018). Strategies for controlling CRISPR/Cas9 off-target effects and biological variations in mammalian genome editing experiments. J. Biotechnol. *284*, 91–101.
30. Vairy, S., Garcia, J.L., Teira, P., and Bittencourt, H. (2018). CTL019 (tisagenlecleucel): CAR-T therapy for relapsed and refractory B-cell acute lymphoblastic leukemia. Drug Des. Dev. Ther. *12*, 3885–3898.
31. Mohty, M., Gautier, J., Malard, F., Aljurf, M., Bazarbachi, A., Chabannon, C., Kharfan-Dabaja, M.A., Savani, B.N., Huang, H., Kenderian, S., et al. (2019). CD19 chimeric antigen receptor-T cells in B-cell leukemia and lymphoma: current status and perspectives. Leukemia *33*, 2767–2778.
32. Maude, S.L., Laetsch, T.W., Buechner, J., Rives, S., Boyer, M., Bittencourt, H., Bader, P., Verneris, M.R., Stefanski, H.E., Myers, G.D., et al. (2018). Tisagenlecleucel in children and young adults with B-cell lymphoblastic leukemia. New Engl. J. Med. *378*, 439–448.
33. Stinchcombe, J.C., Bossi, G., Booth, S., and Griffiths, G.M. (2001). The immunological synapse of CTL contains a secretory domain and membrane bridges. Immunity *15*, 751–761.
34. Finney, O.C., Brakke, H.M., Rawlings-Rhea, S., Hicks, R., Doolittle, D., Lopez, M., Futrell, R.B., Orentas, R.J., Li, D., Gardner, R.A., et al. (2019). CD19 CAR T cell product and disease attributes predict leukemia remission durability. J. Clin. Invest. *129*, 2123–2132.
35. McLellan, A.D., and Ali Hosseini Rad, S.M. (2019). Chimeric antigen receptor T cell persistence and memory cell formation. Immunol. Cel. Biol. *97*, 664–674.
36. Sabatino, M., Hu, J., Sommariva, M., Gautam, S., Fellowes, V., Hocker, J.D., Dougherty, S., Qin, H., Klebanoff, C.A., Fry, T.J., et al. (2016). Generation of clinical-grade CD19-specific CAR-modified CD8+ memory stem cells for the treatment of human B-cell malignancies. Blood *128*, 519–528.
37. Louis, C.U., Savoldo, B., Dotti, G., Pule, M., Yvon, E., Myers, G.D., Rossig, C., Russell, H.V., Diouf, O., Liu, E., et al. (2011). Antitumor activity and long-term fate of chimeric antigen receptor-positive T cells in patients with neuroblastoma. Blood *118*, 6050–6056.
38. Das, R.K., Vernau, L., Grupp, S.A., and Barrett, D.M. (2019). Naïve T-cell deficits at diagnosis and after chemotherapy impair cell therapy potential in pediatric cancers. Cancer Discov. *9*, 492–499.
39. Pauza, M.E., Doumbia, S.O., and Pennell, C.A. (1997). Construction and characterization of human CD7-specific single-chain Fv immunotoxins. J. Immunol. *158*, 3259–3269.
40. Mihara, K., Yanagihara, K., Takigahira, M., Imai, C., Kitanaka, A., Takihara, Y., and Kimura, A. (2009). Activated T-cell-mediated immunotherapy with a chimeric receptor against CD38 in B-cell non-Hodgkin lymphoma. J. Immunother. *32*, 737–743.